

HEAT AND MASS TRANSFER IN POROUS AND DISPERSIVE MEDIA

SIMULATION AND OPTIMIZATION OF AN ORGANIC-IMPURITY OXIDIZATION REACTOR WITH A FIXED POROUS BED AND AN ELECTRIC HEATING ELEMENT

N. N. Gnezdilov, K. V. Dobrego,
I. M. Kozlov, and E. S. Shmelev

UDC 536.46

A reactor for oxidization of low-caloric-value organic impurities contained in the air has been simulated. It comprises a tube with a recuperator, filled with a porous carcass mix, and includes a heating element. The influence of the heating-element placement, the heat losses through the upper cover of the reactor, the flow rate of a gas mixture, and the power of the heater on the maximum temperatures of the porous carcass and the gas and on the concentration of the incompletely oxidized organic impurity at the output of the reactor has been investigated. It is shown that, to burn an impurity completely, it will suffice to heat the gas ΔT_e to 300 K. It has been established that it is best to place a heater at the level of the upper cut of the inner tube of the reactor.

Introduction. The neutralization and removal of contaminating gases is a pressing problem for many mechanical, chemical, and biochemical processes, as well as a number of other technological processes [1, 2]. Such gases can be neutralized by a large number of methods involving sorption, condensation, combustion (including catalytic combustion), membrane separation, chemical and biochemical transformation, and other procedures [1, 2]. The neutralization of gases by sorption calls for the recovery of the properties of sorbents having a limiting service life or the use of new ones. The methods of condensation of volatile organic substances can be used only for removal of specific components of a gas mixture, having a relatively high condensation temperature and present in fairly high concentrations in this mixture [1]. In order that the burning of gases in open flames and furnaces be economically beneficial, it should be conducted in special furnaces or plants. Moreover, some contaminants cannot be burnt in this way. The membrane separation, catalytic oxidation, and chemical (or biological) transformations of impurities are fairly selective and expensive and, therefore, can be used effectively only in particular cases [1, 2].

Volatile organic contaminants, such as phenol, acetone, formaldehyde, and benzene, which occur widely in the air, have a combustion heat sufficient for their effective burning in an inert porous medium (filtrational combustion) [3–6]. Filtrational combustion provides effective heat recirculation in a system and, consequently, an economy in the energy consumed. This combustion can be self-sustaining even in the case of very low concentrations of volatile organic substances (~1 mass %) due to their combustion heat. In [7], the stationary combustion of methane in a porous medium in a recuperative reactor at an equivalent ratio between the gas and air of $\Phi = 0.026$ in the mixture (which is approximately 20 times lower than the combustion threshold under open-flame conditions) was investigated. In [3], a regenerative reactor, in which a filtrational-combustion wave was stabilized in a porous carcass due to the change in the direction of gas filtration, was simulated. Contarin et al. [3] obtained a stable combustion at $\Phi = 0.15$.

The physical aspects of filtrational combustion in an inert porous medium were discussed in [4, 8, 9] and other works. A fundamental feature of this combustion is the internal recirculation of heat in the combustion wave due to the heat transfer between a gas and a porous medium in the region of its preliminary heating. Note that, in practice, in reactors for burning of superpoor fuel mixtures, heat recirculation arises due to the heat exchange between the in-

A. V. Luikov Heat and Mass Transfer Institute, National Academy of Sciences of Belarus, 15 Brovka Str., Minsk, 220072, Belarus; email: nick_gn@itmo.by. Translated from *Inzhenerno-Fizicheskii Zhurnal*, Vol. 79, No. 5, pp. 3–10, September–October, 2006. Original article submitted February 6, 2006.

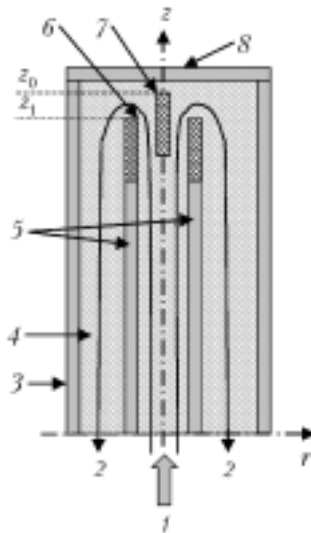


Fig. 1. Diagrams of reactors with different EHEs: 1) inflowing gas mixture; 2) outflowing gases; 3) body of a reactor; 4) porous carcass; 5) inner tube; 6) ring EHE positioned in the upper part of the inner tube; 7) axial EHE; 8) cover of the reactor.

flowing and outflowing gases (recuperative scheme) or due to the change in the gas-filtration direction (regenerative scheme). Such systems were investigated under laboratory conditions in [3, 4, 7, 10, 11] and were used in industrial reactors for oxidization of volatile organic substance of Thermatrix [12], ReEco-Stroem, and other companies [13]. In the reactor simulated in [14], both mechanisms of heat recirculation are combined, which makes it possible to widen its operating range with respect to the concentrations of volatile organic substances and the gas flow rate.

The use of electric heating elements (EHE) in an oxidization reactor makes it possible to remove volatile organic substances from the air without restrictions on their lower concentration and, in the general case, to reliably control the operating temperature conditions of the reactor. This technology is usually used for neutralization of gases with a very low or varying heat capacity and a varying flow rate and in the case where it is necessary to maintain a stable operation of a reactor. Even though electric heating elements are used in such reactors, as the authors know, the influence of the parameters of these elements on the characteristics of a reactor was not investigated theoretically.

In the present work, we investigated the operation of a stationary recuperative reactor with an additional heat supply provided by an EHE and, in particular, the influence of the EHE placement on the thermal efficiency of the reactor and the degree of oxidization of organic substances. The chemical kinetics of oxidization of volatile organic substances was simulated by the gross kinetics of methane oxidization.

Physical Formulation of the Problem. The reactor being considered consists of two coaxial tubes filled with balls representing a porous carcass (Fig. 1). An inflowing poor mixture of methane with air passes through the inner tube and, in doing so, exchanges heat with the porous carcass and is heated. An EHE of power W is positioned at the end of the inner tube. As the gas propagates along the inner tube, its temperature increases due to the recuperative heat flow passing through the tube wall from the outflowing gas, the heat exchange with the porous carcass, and the exothermic reactions. Intensive exothermic processes of oxidization of volatile organic substances begin when the gas temperature reaches 1000 K. It is assumed that the walls of the inner and outer tubes have a zero thickness.

Two cases of arrangement of EHEs were considered: in the first case, an EHE of length 0.2 m and diameter 0.01 m (EHE 6 in Fig. 1) was positioned at the symmetry axis of the reactor, and its upper boundary had a coordinate z_0 ; in the second case, an EHE shaped as a ring of height 0.2 m, thickness 0.005 m, and diameter 0.1 m (EHE 7 in Fig. 1) was mounted in the wall of the inner tube. The EHEs had a zero porosity and exchanged heat only with the porous carcass surrounding them. The parametric investigations of the operation of the reactor were carried out for these two EHEs.

Mathematical Formulation of the Problem. The problem was formulated in the mean-volume approximation. The system of equations being used involves the continuity equations for the gas phase, the gas filtration, the mass of

the chemical gas components, the heat transfer in the porous filling material and in the gas, and the state of an ideal gas [14–16].

$$\frac{\partial \rho_g}{\partial t} + \nabla (\rho_g \mathbf{u}) = 0, \quad (1)$$

$$-\nabla p = \frac{\mu}{k_0} \mathbf{u} + \frac{\rho_g}{k_1} |\mathbf{u}| \mathbf{u}, \quad (2)$$

$$\rho_g \frac{\partial Y_i}{\partial t} + \rho_g \mathbf{u} \nabla Y_i - \nabla \mathbf{s}_i = \dot{\rho}_i, \quad (3)$$

$$\rho_g c_p \frac{\partial T_g}{\partial t} + c_p \rho_g \mathbf{u} \nabla T_g - \nabla \mathbf{q} = \frac{\alpha_{\text{vol}}}{m} (T_s - T_g) - \sum_i h_i \dot{\rho}_i, \quad (4)$$

$$(1 - m) \rho_s c_s \frac{\partial T_s}{\partial t} - \nabla (\lambda \nabla T_s) = \alpha_{\text{vol}} (T_g - T_s) + W_e, \quad (5)$$

$$\rho_g = \frac{pM}{RT_g}. \quad (6)$$

The equation of heat transfer in the gas (4) accounts for the dispersive diffusion and heat conduction, and the equation of heat transfer in the carcass mix (5) includes the radiative heat conduction. The adiabatic boundary conditions are set at the side walls of the reactor. At the upper cover, the adiabatic boundary conditions or the conditions of heat exchange with the environment by Newton's law with a coefficient $\alpha = 6.5 \text{ W}/(\text{m}^2 \cdot \text{K})$ were set. The impermeability conditions were set at the walls of the outer and inner tubes and at the upper cover. The formulation of the problem being considered is described in more detail in [14].

The following standard parameters of the problem were used in calculations: $z_0 = 0.82 \text{ m}$, $z_1 = 0.82 \text{ m}$, $z_2 = 1 \text{ m}$, $d_0 = 1.5 \cdot 10^{-3} \text{ m}$, $d_1 = 0.1 \text{ m}$, $d_2 = 0.16 \text{ m}$, $T_0 = 300 \text{ K}$, $p_0 = 1.01325 \cdot 10^5 \text{ Pa}$, $\varepsilon = 0.35$, $m = 0.5$, $\rho_s = 1750 \text{ kg}/\text{m}^3$, $c_s = 1300 \text{ J}/(\text{kg} \cdot \text{K})$, $\lambda = 0.2 \text{ W}/(\text{m} \cdot \text{K})$, $D_p = 0.5 \text{ m}^{-1}$, $D_\tau = 0.1 \text{ m}^{-1}$, $\Phi = 0.02 \text{ mole}/\text{mole}$, $G = 15 \text{ m}^3/\text{h}$, $U_g = 0.66 \text{ m}/\text{sec}$, $\Delta T_e = 272.5 \text{ K}$.

The case where an EHE was positioned at the axis of the reactor was considered. The combustion of methane was simulated by the gross reaction $\text{CH}_4 + 2\text{O}_2 \xrightarrow{k} \text{CO}_2 + 2\text{H}_2\text{O}$, where $k = 2.17 \cdot 10^8 \exp(-15,640/T_g)$ [17].

Results of Simulation. The main parameters of a reactor for oxidization of volatile organic substances are the maximum temperatures of the gas mixture and the porous medium and the concentration of the incompletely oxidized organic substance at the output of the reactor. As the gas mixture containing a volatile organic substance, we used a methane–air mixture with $\Phi = 0.02$, a mole fraction of methane $X[\text{CH}_4] = 0.001996$, a ratio between the air components $\text{N}_2:\text{O}_2 = 4:1$, a specific combustion heat $\Delta H = 5.7 \cdot 10^4 \text{ J}/\text{kg}$, $\Delta T_{\text{ad}} = 53.0 \text{ K}$, a gas density $\rho_g = 1.16 \text{ kg}/\text{m}^3$ at $T_0 = 300 \text{ K}$, and a heat capacity $c_p = 1025 \text{ V}/(\text{kg} \cdot \text{K})$. At standard parameters, the heat-transfer coefficient $\alpha_{\text{vol}} \approx 10^5 \text{ W}/(\text{m}^3 \cdot \text{K})$.

We investigated the influence of the location of the heating region, the heat losses through the reactor cover, and the electric heating power W on the maximum temperatures of the gas $T_{g,\text{max}}$ and the carcass $T_{s,\text{max}}$ and on the methane concentration $X[\text{CH}_4]_{\text{fin}}$ at the output of the reactor. The electric heating power will be characterized by the temperature of heating of the gas ΔT_e , determined as

$$\Delta T_e = \frac{W}{G (c_p \rho_g) |_{T=T_0}}. \quad (7)$$

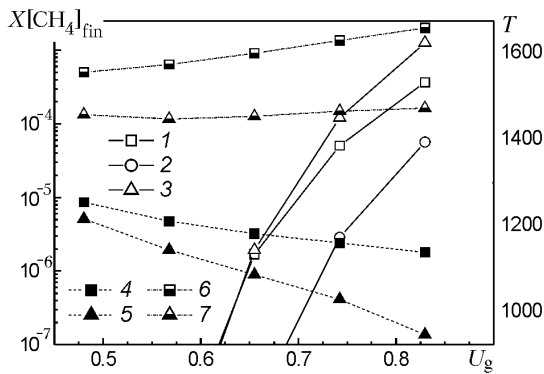


Fig. 2. Dependences of the methane concentration at the output of a reactor $X[\text{CH}_4]_{\text{fin}}$ (1–3) and the maximum temperatures of the gas $T_{g,\text{max}}$ (4, 5) and the porous carcass $T_{s,\text{max}}$ (6, 7) on the gas flow rate U_g determined for inner tubes of different lengths and EHEs of different configurations: 1, 4, 6) $z_1 = 0.82$ m, axial EHE; 2, 4, 6) $z_1 = 0.9$ m, axial EHE; 3, 5, 7) $z_1 = 0.82$ m, ring EHE. U_g , m/sec; $X[\text{CH}_4]_{\text{fin}}$, mole/mole; T , K.

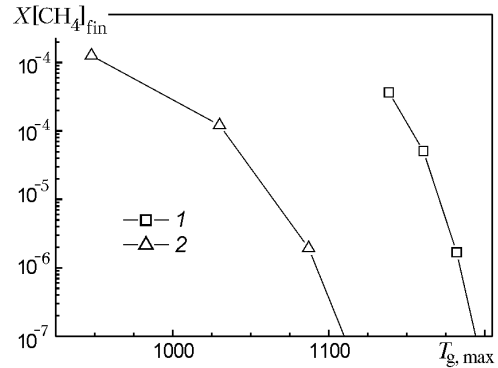


Fig. 3. Correlation of the residual methane concentration $X[\text{CH}_4]_{\text{fin}}$ with the maximum gas temperature $T_{g,\text{max}}$ at a constant temperature ΔT_e : 1) axial EHE; 2) ring EHE. $T_{g,\text{max}}$, K; $X[\text{CH}_4]_{\text{fin}}$, mole/mole.

Problem (1)–(6) was solved using the 2DBurner software package for simulation of nonstationary two-dimensional processes [16]. The parameters of the stable regime of operation of the reactor were used for construction of the desired dependences.

Variable gas flow rate at a constant electric heating temperature. A change in the gas flow rate, at constant other parameters of the process being considered, leads to a change in the position of the combustion front and to the corresponding thermal transformation of the system. To maintain the constant heating temperature $\Delta T_e = 272.5$ K, we changed the power of the EHE.

Figure 2 shows the dependences of $X[\text{CH}_4]_{\text{fin}}$, $T_{g,\text{max}}$, and $T_{s,\text{max}}$ on the gas flow rate U_g for inner tubes of different lengths and for EHEs of different configurations. Since, for these tubes, the temperatures $T_{g,\text{max}}$ and $T_{s,\text{max}}$ are practically equal, we present the temperatures $T_{g,\text{max}}$ (curve 4) and $T_{s,\text{max}}$ (curve 6) only for the inner tube of standard length $z_1 = 0.82$ m. As follows from Fig. 2, at $\Delta T_e = \text{const}$, the maximum temperature of the gas insignificantly decreases (curves 4 and 5) and the maximum temperature of the carcass increases (curves 6 and 7) with increase in the gas flow rate. This is explained by the fact that the EHE heat is transferred only through the porous carcass, which is why the temperature of the EHE increases with increase in the power W . However, the coefficient of three-dimensional heat transfer, included in (4) and (5), is determined as $\alpha_{\text{vol}} \approx \text{Re}^{0.6}$ [14, 16] and, therefore, the density of the heat flow passing from the porous carcass to the gas increases more slowly than the gas flow rate, which leads to a decrease in the maximum gas temperature. Clearly, in the case where the EHE power is constant, both $T_{g,\text{max}}$ and $T_{s,\text{max}}$ decrease with increase in the gas flow rate. Variations in the design parameters of the reactor, such as the length of the inner tube and the placement of the EHE, substantially influence the regime of its operation. In Fig. 2, we present, for comparison, the dependences of the residual methane concentration (curves 1 and 2) and the maximum temperatures of the gas (curve 4) and the porous carcass (curve 5) on the gas flow rate at $z_1 = 0.82$ and 0.9 m. It is seen that an increase in the length of the inner tube insignificantly influences the above-indicated maximum temperatures and substantially (by an order of magnitude) decreases the methane concentration at the output of the system, which is explained by the increase in the distance at which the heated gas mixture is burnt completely.

It is seen from the graphs presented in Fig. 2 that, in the case where an axial EHE is used, the maximum temperature of the gas is much higher and the residual methane concentration is lower at $U_g > 0.66$ m/sec. The results obtained indicate that the use of such an EHE is more appropriate from the standpoint of attainment of a maximum gas temperature; however, in this case, the temperature field in the combustion region is more inhomogeneous than in the case where a ring EHE is used and a part of the gas filtrated through the low-temperature zones remains incom-

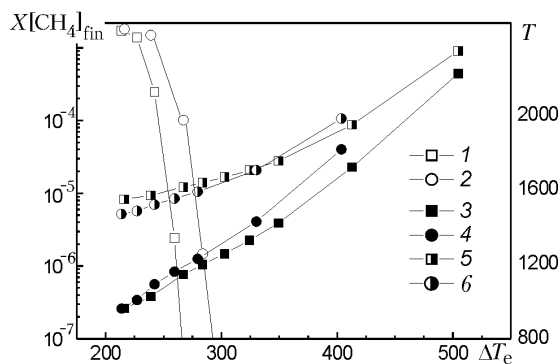


Fig. 4. Dependences of the methane concentration at the output of the reactor $X[\text{CH}_4]_{\text{fin}}$ (1, 2) and the maximum temperatures of the gas $T_{g,\text{max}}$ (3, 4) and the porous carcass $T_{s,\text{max}}$ (5, 6) on the temperature of heating of the gas mixture ΔT_e : 1, 3, 5) $W = 1200$; 2, 4, 6) 1500 W. ΔT_e , K; $X[\text{CH}_4]_{\text{fin}}$, mole/mole; T , K.

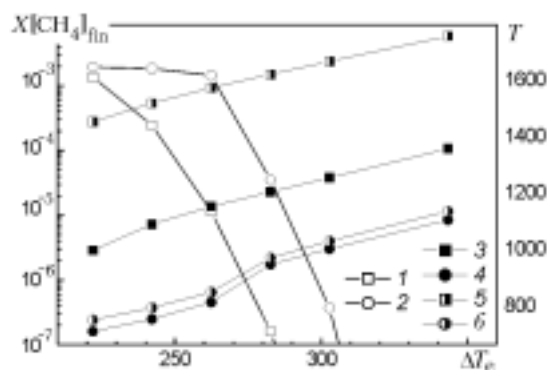


Fig. 5. Dependences of the methane concentration at the output of the reactor $X[\text{CH}_4]_{\text{fin}}$ (1, 2) and the maximum temperature of the gas $T_{g,\text{max}}$ (3, 4) and the porous carcass $T_{s,\text{max}}$ (5, 6) on the temperature of heating of the gas mixture ΔT_e : 1, 3, 5) axial EHEs; 2, 4, 6) ring EHEs. $U_g = 0.66$ m/sec; ΔT_e , K; $X[\text{CH}_4]_{\text{fin}}$, mole/mole; T , K.

pletely oxidized. This feature is illustrated by curves 1 and 2 in Fig. 3, representing correlations of the residual methane concentration with the maximum gas temperature for the axial and ring EHEs at a constant ΔT_e . It is seen that the gas flow rate U_g decreases with increase in the maximum gas temperature.

Thus, it is advantageous to use an axial EHE in a reactor of the type being considered if the flow rate of a gas in it is high, because the obtaining of a low residual organic-substance concentration at the output of this reactor is a fundamental requirement imposed upon it.

Constant power W of an EHE. The regime of operation of the reactor being considered at a constant power of an EHE is more simple from the engineering standpoint. In this case, the parametric dependences somewhat differ from the analogous dependences for the regime with a constant specific energy supplied (Figs. 2 and 3). Figure 4 shows the dependences of $X[\text{CH}_4]_{\text{fin}}$, $T_{g,\text{max}}$, and $T_{s,\text{max}}$, calculated for two EHE powers, 1200 and 1500 W, on ΔT_e determined from (7). It is seen from this figure that, at one and the same heating temperature, the methane concentration at the output of the reactor is lower in the case where the heating power is smaller, i.e., where $W = 1200$ W, even though the maximum temperature of the gas is also lower in this case. This is due to the inhomogeneous heating of the gas flow in the region of the EHE. Therefore, at the thermophysical parameters being used, the methane impurity is effectively removed from the gas mixture at a gas flow rate $U_g = 0.66$ m/sec and a heating temperature $\Delta T_e \approx 275$ K.

Heating at a constant gas flow rate. A number of parametric dependences were obtained at a constant gas flow rate $U_g = 0.66$ m/sec. Figure 5 shows the dependences of $X[\text{CH}_4]_{\text{fin}}$, $T_{g,\text{max}}$, and $T_{s,\text{max}}$ on the heating temperature ΔT_e in the cases where the axial or the ring EHE is used. It follows from Fig. 5 that, when the ring EHE is used, methane burns at $\Delta T_e \approx 260$ K: this temperature is approximately 40 K higher than the analogous temperature in the case where the axial EHE is used. This is evidenced by the sharp decrease in the methane concentration at the output from the reactor (curve 2) and the increase in the maximum temperatures of the gas and the porous carcass (curves 4 and 6).

Comparison of the characteristics (Fig. 5) obtained for the cases where the axial (curve 1) or ring (curve 2) EHE is used shows that, in the first case, methane begins to burn at a lower heating temperature ΔT_e . Thus, at a constant heating temperature ΔT_e , as at a constant power W , the use of an axial EHE is preferential. In this case, the maximum temperature of the gas is higher and methane burns more completely and at a lower temperature ΔT_e than in the case where a ring EHE is used. However, as was noted above, the temperature distribution over the cross sec-

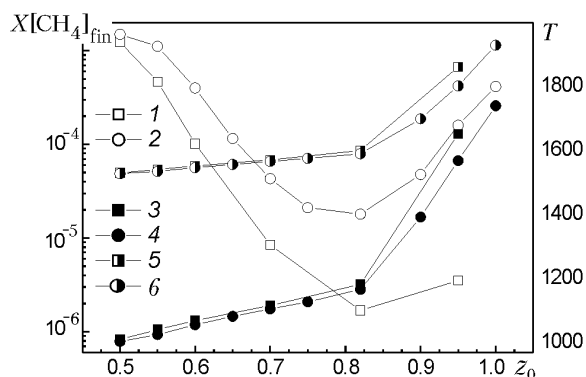


Fig. 6. Dependences of the methane concentration at the output of the reactor $X[\text{CH}_4]_{\text{fin}}$ (1, 2) and the maximum temperatures of the gas $T_{g,\text{max}}$ (3, 4) and the porous carcass $T_{s,\text{max}}$ (5, 6) on the coordinate z_0 of the EHE: 1, 3, 5) adiabatic reactor; 2, 4, 6) reactor with a nonisolated upper cover. z_0 , m; $X[\text{CH}_4]_{\text{fin}}$, mole/mole; T , K.

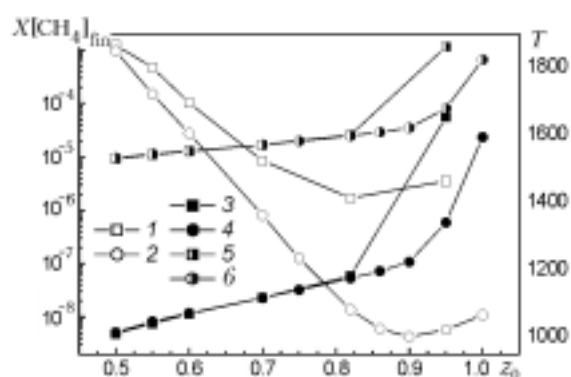


Fig. 7. Dependences of the methane concentration at the output of the reactor $X[\text{CH}_4]_{\text{fin}}$ (1, 2) and the maximum temperatures of the gas $T_{g,\text{max}}$ (3, 4) and the porous carcass $T_{s,\text{max}}$ (5, 6) on the coordinate z_0 of the EHE determined for inner tubes of different lengths: $z_1 = 0.82$ (1, 3, 5) and 0.9 m (2, 4, 6). z_0 , m; $X[\text{CH}_4]_{\text{fin}}$, mole/mole; T , K.

tion of the gas flow in the reactor with an axial EHE is not so inhomogeneous as that in the reactor with a ring EHE, which leads to a relatively large increase in $X[\text{CH}_4]_{\text{fin}}$ at one and the same values of $T_{g,\text{max}}$.

Efficiency of work of an EHE depending on the heat insulation of the reactor. The efficiency of work of an EHE depends on its placement in a reactor and the length of the reactor inner tube. To determine the dependence of the optimum placement of an EHE on the heat losses through the upper cover of a reactor (see Fig. 1), we calculated a number of reactors with axial EHEs positioned differently and with an adiabatic upper cover or a nonadiabatic cover exchanging heat with the environment ($T_0 = 300$ K) by Newton's law with a heat-transfer coefficient of $6.5 \text{ W}/(\text{m}^2 \cdot \text{K})$. The results of these calculations are presented in Fig. 6. Figure 7 illustrates the influence of the placement of an EHE on $X[\text{CH}_4]_{\text{fin}}$, $T_{g,\text{max}}$, and $T_{s,\text{max}}$ in reactors with inner tubes of length 0.82 and 0.9 m.

As is seen from Figs. 6 and 7, in the case where an EHE is positioned within the inner tube of a reactor, i.e., when $z_0 \leq z_1$, the appearance of heat losses and an increase in the length of the inner tube lead to a significant change in the maximum temperatures of the gas $T_{g,\text{max}}$ and the carcass $T_{s,\text{max}}$, as compared to those in the standard case. However, due to the heat losses through the upper cover, the curve of the methane residual concentration $X[\text{CH}_4]_{\text{fin}}$ (curve 2 in Fig. 6) lies higher than that in the standard case (curve 1). This incomplete combustion of methane is due to the cooling of the reactor region located near the upper cover. An increase in the length of the inner tube leads to a decrease in the methane concentration at the output of the reactor (Fig. 7, curve 2), as compared to that in the standard case (curve 1), which can be explained only by the longer time of residence of the gas in the hot region. The smooth increase in the maximum temperatures of the gas and the carcass (curves 3–6 in Figs. 6 and 7) is due to the increase in the recuperation length (it can be assumed to be equal to z_0), along which the outflowing heated gas transfers its heat to the cold gas inflowing through the inner tube.

When the coordinate of an axial EHE further increases ($z_0 > z_1$), the temperatures $T_{g,\text{max}}$ and $T_{s,\text{max}}$ begin to grow (Figs. 6 and 7). This is explained by the fact that the EHE part located above the inner tube is in the stagnation region in which there is practically no heat exchange with the gas, which leads to a strong inhomogeneous heating of the system. A part of the gas passes past the hot region and remains unoxidized, with the result that the methane concentration at the reactor output increases (curves 1 and 2 in Figs. 6 and 7). In the case of heat losses, the maximum temperatures of the gas and the carcass increase more slowly with increase in z_0 than in the standard case (Fig. 6, curves 3–6).

CONCLUSIONS

1. It is advantageous to design recuperative reactors for oxidization of volatile organic substances with an inner tube of maximum length allowed by the reactor design and the requirements imposed upon the pressure difference in it. In this case, large degrees of heat recuperation and volatile-organic-substance oxidization are attained.

2. The axial placement of an EHE inside the tube of a reactor makes it possible to substantially increase the maximum temperature of the gas in it independently of the gas flow rate. However, in this case, a small methane concentration at the output of the reactor is obtained only at large gas flow rates (at $U_g > 0.66$ m/sec for the reactor being considered), and the temperature distributions over the cross section of the carcass and the gas flow are more inhomogeneous than in the case where a ring EHE is used. This fact should be taken into account in designing a reactor if the thermal stability of the porous medium or its resistance to thermal stresses is a critical factor for this reactor.

3. The calculation data obtained allow one to optimize the operating parameters of an oxidization reactor. For example, the optimum temperature of heating ΔT_e of the mixture of methane with air, in which the methane concentration corresponds to $\Phi = 0.02$, is close to 275 K; in this case, the methane concentration at the output of the reactor is $X[\text{CH}_4]_{\text{fin}} \approx 10^{-7}$ mole/mole at a fairly low heating power. The placement of an EHE at the axis of a reactor at a distance equal to the length of its inner tube can be considered as optimum because the residual concentration of hydrocarbons is minimum in this case.

4. In the present work, a model reactor with a large number of constant parameters was considered. To determine the optimum regimes of operation of other reactors for a wide range of concentrations of oxidized substances and for different porous media, it is necessary to perform additional calculations.

This work was carried out with financial support from the Belarusian Republic Basic Research Foundation (project T05-259) and the State Committee on Science and Technology of the Republic of Belarus (project 61).

NOTATION

c_p , heat capacity of a gas at a constant pressure, J/(kg·K); c_s , heat capacity of the porous carcass mix, J/(kg·K); \mathbf{D} , diffusion tensor including the diffusion coefficient of the gas and the dispersive-diffusion tensor (D_p and D_τ are its components); d_0 , diameter of the filling-material particles, m; d_1 , diameter of the inner tube of a reactor, m; d_2 , diameter of the outer tube of the reactor, m; G , gas flow rate, m^3/h ; h_i , mass enthalpy of the i th gas component, J/kg; k_0 , K_1 , Ergun permeability constants; m , porosity; M , mean molar mass of the gas, kg/mole; p , pressure, Pa; p_0 , pressure at the output of the reactor, Pa; \mathbf{q} , conductive heat flux in the gas, $\mathbf{q} = \Lambda \nabla T_g$; r , radial coordinate, m; R , universal gas constant; Re , Reynolds number; S , area of the reactor cross section; \mathbf{s}_i , diffusion flow of the i th chemical element, $\mathbf{s}_i = \rho_g \mathbf{D} \nabla Y_i$; t , time; T_0 , initial temperature of the system, K; T , temperature, K; T_{ad} , adiabatic combustion temperature, K; $\Delta T_{\text{ad}} = T_{\text{ad}} - T_0$; $\Delta T_e = \frac{W}{G(c_p \rho_g)} \Big|_{T=T_0}$, temperature of heating of the gas mixture (the temperature to

which the gas is heated by only an EHE), K; $T_{g,\text{max}}$, maximum gas temperature, K; $T_{s,\text{max}}$, maximum temperature of the porous carcass, K; \mathbf{u} , rate of gas filtration, m/sec; $U_g = G/S$, specific flow rate of the gas, m/sec; W , total power of the EHE, W; W_e , power of the EHE per unit volume, W; Y_i , mass fraction of the i th gas component, kg/kg; z , longitudinal coordinate, m; z_0 , coordinate of the upper boundary of the EHE m; z_1 , length of the inner tube of the reactor, m; z_2 , length of the reactor, m; α and α_{vol} , heat-transfer coefficients, $\text{W}/(\text{m}^2 \cdot \text{K})$ and $\text{W}/(\text{m}^3 \cdot \text{K})$; ε , degree of darkness of the porous carcass; Λ , tensor of gas heat conduction, $\Lambda = c_p \rho_g \mathbf{D}$; λ , effective heat conduction of the porous carcass, $\text{W}/(\text{m} \cdot \text{K})$; μ , viscosity of the gas, Pa·sec; ρ , density, kg/m^3 ; $\dot{\rho}_i$, rate of formation of the i th component as a result of the chemical reactions, kg/sec; Φ , fuel/oxidizer ratio. Subscripts: 1, inner tube; 2, outer tube; ad, adiabatic; e, electric; fin, output parameter; g, gas; i , number of a gas mixture component; max, maximum; s, porous carcass; vol, volumetric.

REFERENCES

1. Selecting the most appropriate HAP emission control technology, *The Air Pollution Consultant*, **3**, Issue 2, 1–9 (1993).

2. Yu. Sh. Matros, A. S. Noskov, and V. A. Chumachenko, *Catalytic Decontamination of Industrial Waste Gases* [in Russian], Nauka, Novosibirsk (1991), pp. 22–37.
3. F. Contarin, A. V. Saveliev, A. A. Fridman, and L. A. Kennedy, A reciprocal flow filtration combustor with embedded heat exchangers: Numerical study, *Int. J. Heat Mass Transfer*, **46**, 949–961 (2003).
4. L. A. Kennedy, A. A. Fridman, and A. V. Saveliev, Superadiabatic combustion in porous media: Wave propagation, instabilities, new type of chemical reactor, *Int. J. Fluid Mech. Res.*, **22**, 1–26 (1995).
5. J. G. Hoffman, R. Echigo, H. Yoshida, and S. Tada, Experimental study on combustion in a porous media with a reciprocating flow system, *Combust. Flame*, **111**, 32–46 (1997).
6. W. D. Binder and R. J. Martin, The destruction of air toxic emissions by flameless thermal oxidation, *Incineration Conf.*, Knoxville, Tennessee (1993).
7. T. Takeno and K. Sato, An analytical study on excess enthalpy flames, *Combust. Sci. Technol.*, **20**, 73 (1979).
8. K. V. Dobrego and S. A. Zhdanok, *Physics of Filtrational Combustion of Gases* [in Russian], A. V. Luikov Heat and Mass Transfer Institute, National Academy of Sciences of Belarus, Minsk (2002).
9. K. Hanamura, R. Echigo, and S. Zhdanok, Superadiabatic combustion in a porous medium, *Int. J. Heat Mass Transfer*, **36**, No. 13, 3201–3209 (1993).
10. M. K. Drayton, A. V. Saveliev, L. A. Kennedy, A. A. Fridman, and Y. E. Li, Superadiabatic partial oxidation of methane in reciprocal and counterflow porous burners, in: *Proc. 27th Int. Symp. on Combustion*, Pittsburgh, PA (1998), pp. 1361–1367.
11. A. N. Migoun A. N., A. P. Chernukho, and S. A. Zhdanok, Numerical modeling of reverse-flow catalytic reactor for methane partial oxidation, in: *Proc. Vth Int. School-Seminar "Nonequilibrium Processes and Their Applications,"* Minsk (2000), pp. 131–135.
12. <http://www.thermatrix.com>
13. <http://www.eco-web.com>
14. K. V. Dobrego, N. N. Gnesdilov, I. M. Kozlov, V. I. Bubnovich, and H. A. Gonzalez, Numerical investigation of the new regenerator-recuperator scheme of VOC oxidizer, *Int. J. Heat Mass Transfer*, **48**, 4695–4703 (2005).
15. K. V. Dobrego, I. M. Kozlov, S. A. Zhdanok, and N. N. Gnesdilov, Modeling of diffusion filtration combustion radiative burner, *Int. J. Heat Mass Transfer*, **44**, 3265–3272 (2001).
16. K. V. Dobrego, I. M. Kozlov, N. N. Gnesdilov, and V. V. Vasiliev, *2D Burner — Software Package for Gas Filtration Combustion Systems Simulation and Gas Non-Steady Flames Simulation*, Preprint No. 1 of the A. V. Luikov Heat and Mass Transfer Institute, Minsk (2004).
17. V. Ya. Basevich, A. A. Belyaev, and S. M. Frolov, "Global" kinetic mechanisms for calculation of turbulent reacting flows. Pt. 1. Basic chemical process of heat release, *Khim. Fiz.*, **17**, No. 9, 117–129 (1998).